5704 *Chem. Mater.* **2009,** *21,* 5704–5710
DOI:10.1021/cm9011525

CHEMISTRY OF MATERIALS
Article

# Protein-Mediated Layer-by-Layer Syntheses of Freestanding Microscale Titania Structures with Biologically Assembled 3-D Morphologies

Yunnan Fang,[†] Qingzhong Wu,[†] Matthew B. Dickerson,[†,‡] Ye Cai,[†] Samuel Shian,[†,§] John D. Berrigan,[†] Nicole Poulsen,[§] Nils Kröger,[†,§] and Kenneth H. Sandhage*[,†,§]

[†]*School of Materials Science and Engineering, Georgia Institute of Technology, 771 Ferst Drive, Atlanta, Georgia 30332-0400,* [‡]*Materials and Manufacturing Directorate, Air Force Research Laboratory, Wright-Patterson Air Force Base, Ohio 45433-7702, and* [§]*School of Chemistry and Biochemistry, Georgia Institute of Technology, 801 Atlantic Drive, Atlanta, Georgia 30332-0400*

*Received April 26, 2009. Revised Manuscript Received September 22, 2009*

A simple protein-mediated approach for preparing freestanding (silica free) microscale titania structures with morphologies inherited from complex-shaped, three-dimensional (3-D) biosilica templates (diatom frustules) is demonstrated. The silica diatom frustules were exposed in a repetitive alternating fashion to a silica-binding, titania-forming protein (protamine) and then to an aqueous titania precursor to build up a conformal titania-bearing coating. After organic pyrolysis at 500 °C, the conformal, continuous nature of the resulting crystalline anatase titania coating was confirmed by (i) demonstrating that a titania-coated frustule acted as a sensitive electrochemical hydrogen detector and (ii) selectively removing the silica templates to yield freestanding titania structures that retained the 3-D diatom frustule shape.

## Introduction

Titanium dioxide, $TiO_2$, possesses attractive chemical, electrochemical, biochemical, and optical properties that have led to its widespread use in a variety of applications (catalysts, gas sensors, medical implants, pigments, cosmetics/sunscreens, interference coatings).[1] The scalable syntheses of nanostructured titania microassemblies with tailored morphologies is highly desired for a number of existing and future applications.[2] As a result, several synthetic approaches are being explored for the self-assembly of nanostructured titania.[3] However, such synthetic self-assembly approaches are generally not capable of providing complex three-dimensional (3-D) structures with a wide variety of selectable intricate morphologies.

Biomineral-forming organisms have been found to exhibit an impressive capability for the self-assembly of inorganic structures with complex morphologies and organized micro-to-nanoscale features.[4] For example, the nanostructured silica cell walls (frustules) generated by diatoms (microscopic unicellular algae) possess unique 3-D shapes and patterned nanoscale features (e.g., pores, channels, protuberances) that are faithfully preserved upon biological reproduction. Hence, sustained reproduction of a given diatom species can generate enormous numbers of 3-D frustule replicas.[5] The species-specific

*To whom correspondence should be addressed. E-mail: ken.sandhage@mse.gatech.edu.

(1) (a) Linsebigler, A. L.; Lu, G. Q.; Yates, J. T. *Chem. Rev.* **1995**, *95*, 735–758. (b) Shimizu, Y. *Chem. Sens.* **2002**, *18*, 42–54. (c) Gouma, P. I.; Mills, M. J.; Sandhage, K. H. *J. Am. Ceram. Soc.* **2002**, *83*, 1007–1009.(d) Kokubo, T.; Takadama, H.; Matsushita, T. In *Bioceramics and Their Clinical Applications*; Woodhead Publishing: Cambridge, UK, 2008; pp 485−500. (e) Knauth, P.; Bouchet, R.; Schaf, O.; Weibel, A.; Auer, G. In *Synthesis, Functionalization and Surface Treatment of Nanoparticles*; American Scientific Publishers: Stevenson Ranch, CA, 2003; pp 127−146. (f) Holtzen, D. A.; Reid, A. H. In *Coloring of Plastics*; John Wiley & Sons: Hoboken, NJ, 2004; pp 146−158. (g) Nohynek, G. J.; Lademann, J.; Ribaud, C.; Roberts, M. S. *Crit. Rev. Toxicol.* **2007**, *37*, 251–277. (h) Chen, D.; Yan, Y.; Westenberg, E.; Niebauer, D.; Sakaitani, N.; Chaudhuri, S. R.; Sato, Y.; Takamatsu, M. J. *Sol−Gel Sci. Technol.* **2000**, *19*, 77–82.

(2) (a) Wijnhoven, J. E. G. J.; Vos, W. L. *Science* **1998**, *281*, 802–804. (b) Akin, F. A.; Zreiqat, H.; Jordan, S.; Wijesundara, M. B. J.; Hanley, L. *J. Biomed. Mater. Res.* **2001**, *57*, 588–596. (c) Adachi, M.; Jiu, J.; Isoda, S. *Curr. Nanosci.* **2007**, *3*, 285–295. (d) Passinger, S.; Saifullah, M. S. M.; Reinhardt, C.; Subramanian, K. R. V.; Chichkov, B. N.; Welland, M. E. *Adv. Mater.* **2007**, *19*, 1218–1221.

(3) (a) Peng, J.; Knoll, W.; Park, C.; Kim, D. H. *Chem. Mater.* **2008**, *20*, 1200–1202. (b) Yang, C.; Yang, Z.; Gu, H.; Chang, C. K.; Gao, P.; Xu, B. *Chem. Mater.* **2008**, *20*, 7514–7520. (c) Zhang, Y.; Feng, X.; Liu, H.; Wang, C.; Liu, J.; Wei, Y. *Chem. Lett.* **2008**, *37*, 1264–1265. (d) Mao, Y.; Kanungo, M.; Hemraj-Benny, T.; Wong, S. S. *J. Phys. Chem. B* **2006**, *110*, 702–710. (e) Yu, K.; Zhao, J.; Zhao, X.; Ding, X.; Zhu, Y.; Wang, Z. *Mater. Lett.* **2005**, *59*, 2676–2679. (f) Mor, G. K.; Varghese, O. K.; Paulose, M.; Shankar, K.; Grimes, C. A. *Sol. Energy Mater. Sol. Cells* **2006**, *90*, 2011–2075. (g) Polleux, J.; Pinna, N.; Antonietti, M.; Hess, C.; Wild, U.; Schloegl, R.; Niederberger, M. *Chem.-A Euro. J.* **2005**, *11*, 3541–3551. (h) Sui, X.; Chu, Y.; Xing, S.; Yu, M.; Liu, C. *Colloids Surf., A: Physicochem. Eng. Aspects* **2004**, *251*, 103–107.

(4) (a) Faivre, D.; Schueler, D. *Chem. Rev.* **2008**, *108*, 4875–4898. (b) Cusack, M.; Freer, A. *Chem. Rev.* **2008**, *108*, 4433–4454. (c) Currey, J. D. *Science* **2005**, *309*, 253–254. (d) Bauerlein, E. *Angew. Chem., Int. Ed.* **2003**, *42*, 614–641. (e) Aizenberg, J.; Tkachenko, A.; Weiner, S.; Addadi, L.; Hendler, G. *Nature* **2001**, *412*, 819–822. (f) Mann, S.; Ozin, G. *Nature* **1996**, *382*, 313–318.

(5) (a) Round, F. E.; Crawford, R. M.; Mann, D. G. In *The Diatoms: Biology and Morphology of the Genera*; Cambridge University Press: New York, NY, 1990. (b) Hildebrand, M. *Chem. Rev.* **2008**, *108*, 4855–4874. (c) Hildebrand, M.; Wetherbee, R. In *Progress in Molecular and Subcellular Biology*; Springer-Verlag: Berlin, 2003; Vol. *33*, p 11. (d) Duerr, E. O.; Molnar, A.; Sato, V. *J. Mar. Biotechnol.* **1998**, *7*, 65. (e) Kröger, N.; Poulsen, N. *Ann. Rev. Gen.* **2008**, *42*, 83–107. (f) Hildebrand, M. *Chem. Rev.* **2008**, *108*, 4855–4874.

 Published on Web 11/20/2009 

(genetic) control over the biosilicification process also results in a large variety of frustule morphologies among the $10^4-10^5$ extant diatom species.[5] Given such massively parallel and genetically precise 3-D self-assembly, several authors have explored the shape-preserving chemical modification of diatom frustules.[6,7] For example, the microscopic $SiO_2$-based structures (frustules) formed by diatoms have been converted into MgO, Si, $TiO_2$, and $ZrO_2$ replicas via the use of gas/solid displacement reactions.[6] However, such chemical conversion requires the use of reactant species capable of undergoing thermodynamically favored reactions with the relatively stable oxide, silica. Diatom frustules may also be chemically modified via application of functional inorganic coatings. For example, thin coatings of Au, $SnO_2$, and $TiO_2$ have been applied to 3-D diatom frustule surfaces via use of complementary oligonucleotide strands as binding agents, surface sol−gel processing, and atomic layer deposition, respectively.[7] However, these approaches have involved the use of prolonged, multistep surface functionalization protocols or specialized equipment.

An alternative approach (first discussed in a published U.S. Patent application[8]) would be to utilize multifunctional biomolecules to generate conformal coatings on diatom silica frustules, by taking advantage of both silica-binding and oxide-forming capabilities. Particular peptides or proteins have been found to exhibit a high affinity for silica.[9] For example, silaffins (diatom proteins) are capable of inducing the formation of silica and becoming intimately intermixed with such silica, under ambient conditions.[9b,d] Recent work has also shown that a recombinant silaffin, rSilC (a 17.6 kDa lysine and arginine rich (27%) protein), is capable of inducing the formation of rutile titania upon exposure to the titania precursor, TiBALDH (titanium(IV) bis(ammonium lactato)dihydroxide).[9d] Other lysine and arginine-bearing peptides or proteins have also been found to induce the formation of amorphous silica and amorphous or partially nanocrystalline (anatase) titania from aqueous precursor solutions.[9d,10] Indeed, recent systematic work by Dickerson et al.[10d] has revealed that the amount of titania precipitated from a TiBALDH precursor solution by 12-mer peptides was strongly dependent on the presence of a high percentage of arginine and/or lysine residues. Hence, arginine/lysine-rich peptides/proteins exhibit multifunctional (silica binding, titania binding, titania forming) characteristics that may be utilized for the sequential deposition and buildup of a conformal and continuous titania coating on biosilica templates.

The work presented here demonstrates a simple layer-by-layer, protein-mediated approach for generating conformal and continuous titania coatings on, and then freestanding titania replicas of, complex 3-D diatom silica frustule templates. While prior authors have utilized biomolecules and naturally occurring molecules to aid in the deposition of inorganic materials onto diatom frustules,[7a,11] this work provides the first demonstration of freestanding (silica free) replicas of diatom frustules generated via layer-by-layer deposition using multifunctional proteins. The continuous and conformal nature of titania coatings produced by this simple protein-based layer-by-layer process has also enabled the conversion of single diatom frustules into minimally invasive hydrogen detectors.

## Experimental Section

*Aulacoseira* diatom frustules (obtained as diatomaceous earth) were subjected to a two-step cleaning process. The frustules were first exposed to a solution of 50 vol% concentrated (12.1 N) HCl in methanol for 1 h. The frustules were then exposed to a solution composed of DI water, concentrated (30%) $NH_4OH$, and concentrated (30%) $H_2O_2$ in a volume ratio of 4.7:1:1 (RCA-1 cleaning procedure[12]) for 1 h at 75 °C. After rinsing with a 20 mM Tris−HCl (pH 7.5) buffer solution, the diatom frustules were incubated with a solution of protamine sulfate (10 mg/mL, Sigma Aldrich, Milwaukee, WI, Cat. No. P4020) in the Tris−HCl buffer for 1 h at room temperature (Step 1 in Scheme 1) to allow for protamine binding to the silica surface. The protamine-treated diatom frustules were rinsed five times with the Tris−HCl buffer and then exposed (Step 2) to a solution of 50 mM TiBALDH in 20 mM Tris−HCl for 15 min at room temperature to allow for protamine-induced titania formation on the frustule surfaces. After washing five times with the Tris−HCl buffer, the frustules were re-exposed (Step 3) to the protamine sulfate solution to bind additional protamine to the titania-bearing frustules surfaces. Such cyclic exposure to

(6) (a) Sandhage, K. H.; Dickerson, M. B.; Huseman, P. M.; Caranna, M. A.; Clifton, J. D.; Bull, T. A.; Heibel, T. J.; Overton, W. R.; Schoenwaelder, M. E. A. *Adv. Mater.* **2002**, *14*, 429–433. (b) Unocic, R. R.; Zalar, F. M.; Sarosi, P. M.; Cai, Y.; Sandhage, K. H. *Chem. Commun.* **2004**, 795–796. (c) Cai, Y.; Allan, S. M.; Zalar, F. M.; Sandhage, K. H. *J. Am. Ceram. Soc.* **2005**, *88*, 2005–2010. (d) Shian, S.; Cai, Y.; Weatherspoon, M. R.; Allan, S. M.; Sandhage, K. H. *J. Am. Ceram. Soc.* **2006**, *89*, 694–698. (e) Lee, S. J.; Shian, S.; Huang, Ch.-H.; Sandhage, K. H. *J. Am. Ceram. Soc.* **2007**, *90*, 1632–1636. (f) Bao, Z.; Weatherspoon, M. R.; Cai, Y.; Shian, S.; Graham, P. D.; Allan, S. M.; Ahmad, G.; Dickerson, M. B.; Church, B. C.; Kang, Z.; Summers, C. J.; Abernathy, H. W.III; Liu, M.; Sandhage, K. H. *Nature* **2007**, *446*, 172–175. (g) Bao, Z.; Ernst, E. M.; Yoo, S.; Sandhage, K. H. *Adv. Mater.* **2009**, *21*, 474–478.

(7) (a) Rosi, N. L.; Thaxton, C. S.; Mirkin, C. A. *Angew. Chem., Int. Ed.* **2004**, *43*, 5500–5503. (b) Weatherspoon, M. R.; Dickerson, M. B.; Wang, G.; Cai, Y.; Shian, S.; Jones, S. C.; Marder, S. R.; Sandhage, K. H. *Angew. Chem., Int. Ed.* **2007**, *46*, 5724–5727. (c) Losic, D.; Triani, G.; Evans, P. J.; Atanacio, A.; Mitchell, J. G.; Voelcker, N. H. *J. Mater. Chem.* **2006**, *16*, 4029–4034.

(8) Dickerson, M. B.; Sandhage; K. H.; Naik, R.; Stone, M. O. U.S. Patent App. 20070112548 May 17, **2007**.

(9) (a) Shimzu, K.; Cha, J.; Stucky, G. D.; Morse, D. E. *Proc. Natl. Acad. Sci. U.S.A.* **1998**, *95*, 6234–6238. (b) Kröger, N.; Deutzmann, R.; Sumper, M. *Science* **1999**, *286*, 1129–1132. (c) Knecht, M. R.; Wright, D. W. *Chem. Commun.* **2003**, *24*, 3038–3039. (d) Kröger, N.; Dickerson, M. B.; Ahmad, G.; Cai, Y.; Haluska, M. S.; Sandhage, K. H.; Poulsen, N.; Sheppard, V. C. *Angew. Chem., Int. Ed.* **2006**, *45*, 7239–7243. (e) Jiang, Y. J.; Yang, D.; Zhang, L.; Li, L.; Sun, Q. Y.; Zhang, Y. F.; Li, J.; Jiang, Z. Y. *Dalton Trans.* **2008**, *31*, 4165–4171.

(10) (a) Luckarift, H. R.; Dickerson, M. B.; Sandhage, K. H.; Spain, J. C. *Small* **2006**, *2*, 640–643. (b) Sewell, S. L.; Wright, D. W. *Chem. Mater.* **2006**, *18*, 3108–3113. (c) Jiang, Y. J.; Yang, D.; Zhang, L.; Li, L.; Sun, Q. Y.; Zhang, Y. F.; Li, J.; Jiang, Z. Y. *Dalton Trans.* **2008**, *31*, 4165–4171. (d) Dickerson, M. B.; Jones, S. E.; Cai, Y.; Ahmad, G.; Naik, R. R.; Kröger, N.; Sandhage, K. H. *Chem. Mater.* **2008**, *20*, 1578–1584. (e) Dickerson, M. B.; Sandhage, K. H.; Naik, R. R. *Chem. Rev.* **2008**, *108*, 4935–4978.

(11) (a) Jia, Y.; Han, W.; Xiong, G.; Yang, W. *J. Colloid Interface Sci.* **2008**, *323*, 326–31. (b) Jeffryes, C.; Gutu, T.; Jiao, J.; Rorrer, G. L. *J. Mater. Res.* **2008**, *23*, 3255–3262.

(12) Kwietniewski, N.; Sochacki, M.; Szmidt, J.; Guziewicz, M.; Kaminsca, E.; Piotrowska, A. *Appl. Surf. Sci.* **2008**, *254*, 8106–8110.

**Scheme 1. Illustration of the Protein-Enabled Layer-by-Layer Deposition of a Conformal Titania Coating on a Silica-Based Template (such as a diatom frustule)**

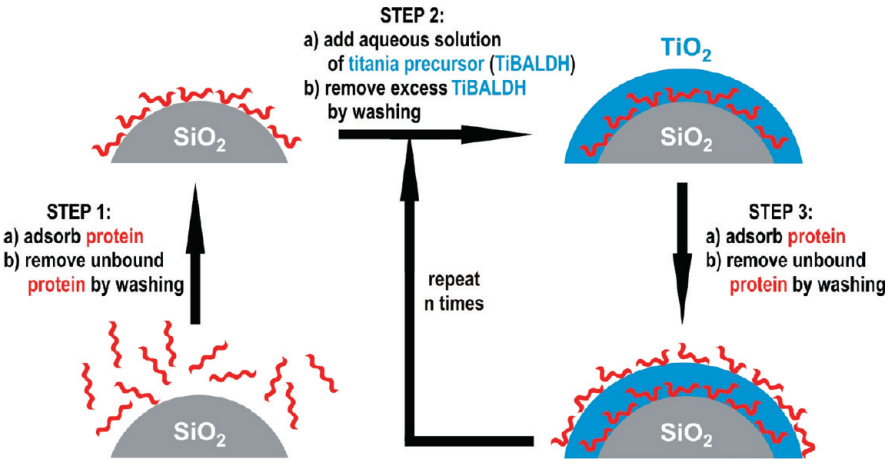


protamine and then TiBALDH was repeated 11 times (for a total of 12 cycles). Two control experiments were also conducted to evaluate the influence of electrostatic interactions on protamine binding to silica and titania surfaces. For the first control experiment, the pH of the protamine solution in each deposition cycle was lowered to 2.2 with the use of a 20 mM glycine−HCl buffer. For the second control experiment, 1 M NaCl was added to the protamine solution used in each deposition cycle, while maintaining the solution pH at 7.5 (with a Tris−HCl buffer). After the last cycle of the standard and control deposition protocols, the diatom frustule specimens were washed five times with DI water and twice with methanol before drying at room temperature for 30 min in a vacuum centrifuge. The protamine/TiBALDH-treated *Aulacoseira* frustules were heated to 500 °C for 2 h in air to allow for organic pyrolysis and the formation of a nanocrystalline titania coating. After firing, the underlying silica frustule template was removed by selective dissolution in a 5 M NaOH solution at 95 °C for 8 h to yield freestanding titania structures.

Scanning electron microscopy was conducted with a field emission scanning electron microscope (Leo 1530 FEG SEM, Carl Zeiss SMT Ltd., Cambridge, UK) equipped with an energy dispersive X-ray spectrometer (INCA EDS, Oxford Instruments, Bucks, UK). X-ray diffraction (XRD) analyses were conducted with Cu Kα radiation using an X-Pert Pro Alpha 1 diffractometer equipped with an incident beam Johannsen monochromator and an X'Celerator linear detector (PANalytical, Almelo, The Netherlands). X-ray photoelectron spectroscopy (XPS) was performed on a Surface Instruments (SSI) M-probe instrument operated at a base pressure of $3 \times 10^{-7}$ Pa using an Al K-α source (1486.6 eV) and step sizes of 0.01 eV (for high-resolution XPS analysis) and 1 eV (for a general XPS survey). A focused ion beam (FIB) instrument (Model Nova Nanolab 200, FEI, Oregon, USA) was used to generate cross sections of freestanding frustule-shaped titania structures. Ion milled thin foil cross sections of the titania structures were characterized with a transmission electron microscope (Model JEM 4000EX, JEOL, Tokyo, Japan) operated at 400 kV.

For hydrogen gas sensing measurements, a single *Aulacoseira*-shaped, titania-bearing frustule structure was placed on a silicon nitride substrate and platinum electrodes were applied to each end of the cylinder-shaped structure with the aid of a FIB instrument. The electroded frustule-shaped structure was placed within a controlled atmosphere horizontal tube furnace and positioned 2 mm below a nozzle through which a $H_2$-bearing gas stream was passed at a constant flow rate (100 sccm). Controlled $H_2$ concentrations were generated by mixing two streams of gases using mass flow controllers (Model FMA-2617A, Omega, Stamford, CT, USA). One gas stream was composed of a certified premixed 1% $H_2$/99% Ar composition (Air Gas, Atlanta, GA, USA) and the other gas stream consisted of high purity Ar (Air Gas). A constant bias voltage (600 mV) was applied to the sensor, and the current passing through the sensor during exposure to a given hydrogen gas concentration at 350 °C was monitored with a potentiostat (Reference 600, Gamry Instrument, Warminster, PA, USA). The sensing performance of five such single, titania-bearing frustule structures was evaluated.

## Results and Discussion

An underlying hypothesis of the present paper is that the silica binding and titania forming characteristics of arginine/lysine-rich biomolecules can both be utilized to induce the layer-by-layer formation of conformal and continuous titania coatings on complex-shaped 3-D silica templates, so that removal of the underlying silica would yield freestanding titania structures that retain the original 3-D template morphology. Preliminary experiments revealed that freestanding hollow titania spheres could be generated by repeated alternating exposure of Stöber silica spheres to an arginine-rich protein (protamine) or an arginine/lysine-rich protein (rSilC) and TiBALDH (see Scheme 1), firing (for organic pyrolysis and titania crystallization), and then selective silica dissolution. Such a protein-enabled layer-by-layer deposition process was then applied to more complex, 3-D silica-based diatom frustules. Secondary electron images of a complete and partial silica frustule from the diatom *Aulacoseira* are shown in Figure 1A,B, respectively. The *Aulacoseira* frustule possesses a hollow cylindrical shape, with fine pores (several hundred nm in diameter) aligned in rows running along the length of the cylinder and with narrow channels separating finger-like extensions (the finger-like extensions can be seen more clearly in the partial frustule shown in Figure 1B). After 12 cycles of alternating exposure to the protamine and TiBALDH solutions, the frustules retained the same overall morphology as

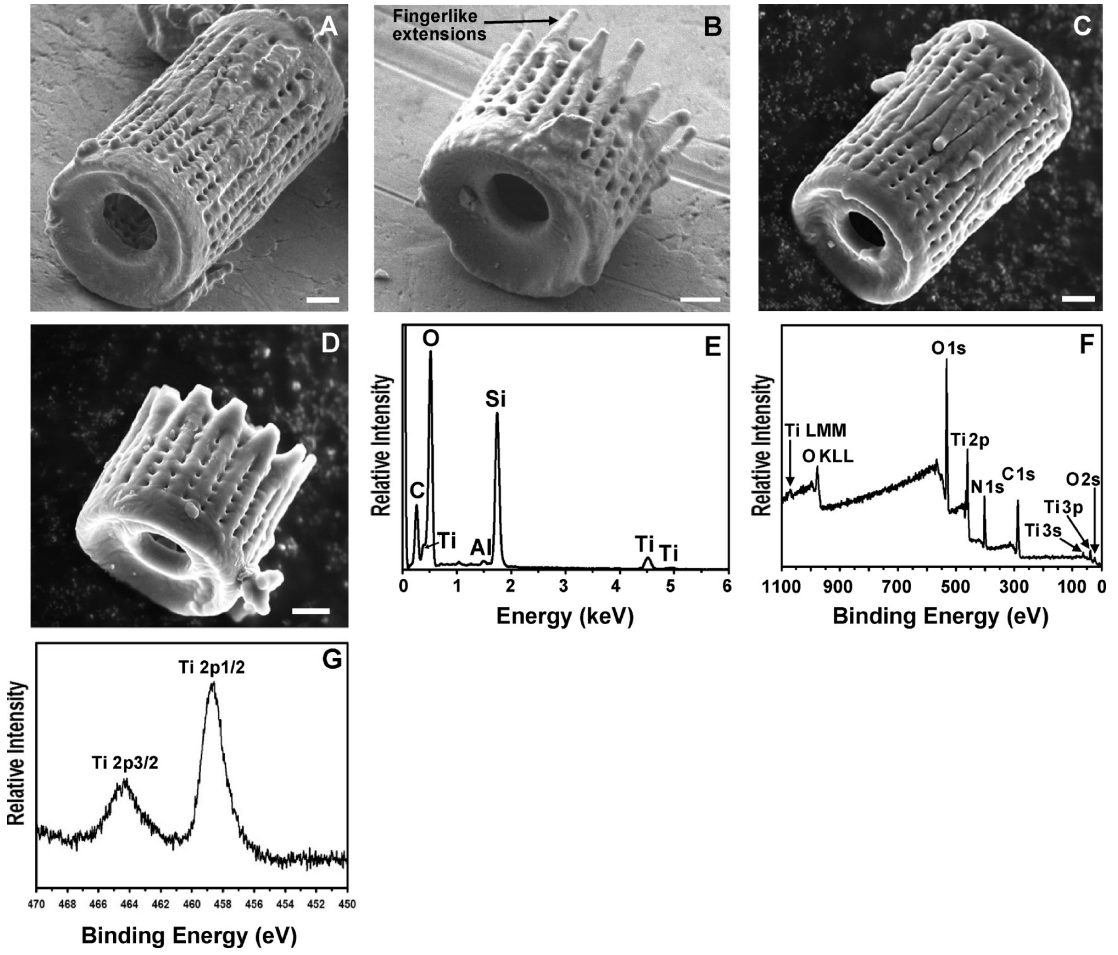


**Figure 1.** Protein-enabled titania coating of *Aulacoseira* diatom frustules. Secondary electron images of (A) and (B) a complete and a partial *Aulacoseira* frustule, respectively, and (C) and (D) a complete and a partial titania-coated *Aulacoseira* frustule, respectively, after 12 cycles of protamine/TiBALDH exposure. Scale bars: 2 $\mu$m. (E) EDX analysis of the specimen in (C). (F) XPS analysis revealing the presence of Ti, O, C, and N, and the absence of Si, on the surfaces of the coated frustules. (G) Higher resolution XPS spectrum from (F) revealing the Ti2p peaks.

the starting frustules (Figure 1C,D) although energy dispersive X-ray (EDX) analysis (Figure 1E) revealed the presence of titanium on these treated frustules. XPS analyses (Figures 1F,G) revealed the presence of Ti, O, N, and C on the protamine/TiBALDH treated frustule surfaces, with the nitrogen and carbon presumably associated with entrapped protamine within the Ti−O-bearing coating. However, the Si 2s peak (at 154 eV) and the Si 2p peak (at 103 eV) were not detected in the XPS pattern of Figure 1F, which indicated that the titanium-bearing coating had completely covered the silica frustule surfaces. The Ti2p3/2 and Ti2p1/2 peaks shown in Figure 1G at binding energies of 458.6 and 464.7 eV, respectively, were consistent with the presence of tetravalent titanium ($TiO_2$) within the coating on the frustules.[13]

The protamine/TiBALDH-treated *Aulacoseira* frustules were heated to 500 °C in air, to allow for organic pyrolysis, and the silica frustule template was then selectively dissolved by exposure to a NaOH solution. Secondary electron images (Figure 2A,C) and EDX analysis (Figure 2B) indicated that the resulting structures were composed of titanium and oxygen, that the silica had been selectively removed, and that such freestanding titania structures retained the 3-D morphology of the starting frustules. (Note: the carbon peak in Figure 2B was associated with the carbon tape on which the sample was placed.) Focused ion beam milling was used to generate cross sections through the frustule-shaped structures by removing some of the titania from one end. A secondary electron image after such partial ion milling (Figure 2D) revealed that the titania structure consisted of continuous external and internal titania layers with a hollow space in between, which resulted from the removal of the silica template. The external and internal titania layers were connected by titania struts formed upon coating of the walls of the pores running through the silica frustule. The images in Figure 2C,D also confirmed the 3-D conformal nature of the coating process; that is, exposed internal and external surfaces of the frustules were covered with a continuous titania coating.

The phase content of the coated frustules was evaluated with X-ray diffraction (XRD), selected area electron diffraction (SAED), and high resolution transmission

(13) (a) Gonbeau, D.; Guimon, C.; Pfister-Guillouzo, G.; Levasseur, A.; Meunier, G.; Dormoy, R. *Surf. Sci.* **1991**, *254*, 81–89. (b) Levin, M. E.; Salmeron, M.; Bell, A. T.; Somorjai, G. A. *Surf. Sci.* **1988**, *195*, 429–442. (c) Ocal, C.; Ferrer, S. *Surf. Sci.* **1987**, *191*, 147–156.

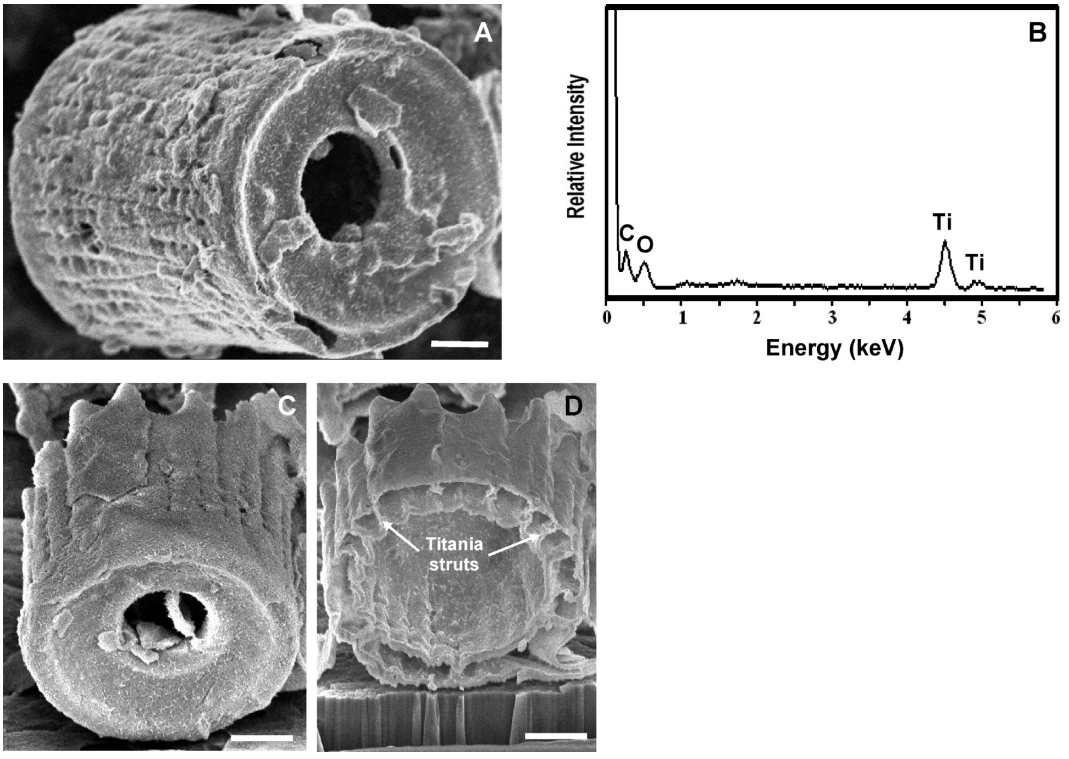


**Figure 2.** Freestanding frustule-shaped titania structures. Secondary electron images of (A) a complete and (C) a partial frustule-derived titania structure, respectively, after 12 cycles of protamine/ TiBALDH exposure, 500 °C/2 h treatment, and selective silica dissolution. (B) EDX analysis of the specimen in (A). (D) The specimen in (C) after partial ion milling. Scale bars: 2 $\mu$m.

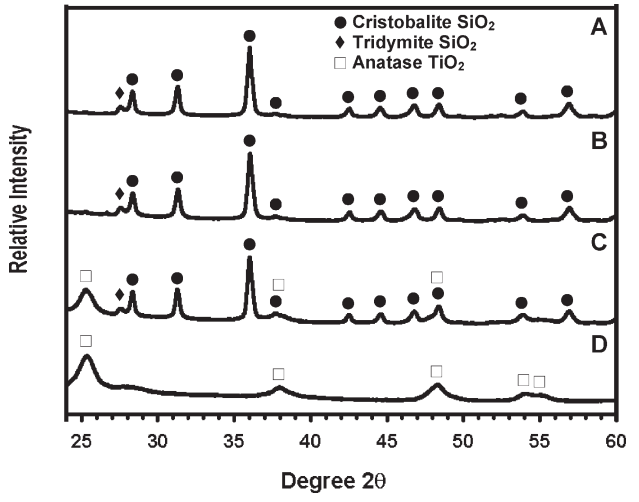


**Figure 3.** Phase content of *Aulacoseira* diatom frustules and their derivatives. XRD analyses of (A) starting silica-based *Aulacoseira* diatom frustules, (B) as-coated diatom frustules (after 12 protamine/TiBALDH cycles), (C) titania-coated diatom frustules after coating and firing at 500 °C for 2 h, and (D) titania-coated diatom frustules after coating, 500 °C/2 h firing, and selective silica dissolution in a NaOH solution.

electron microscope (TEM) analyses. The starting frustules (obtained as flame-polished diatomaceous earth) exhibited XRD peaks for cristobalite and tridymite $SiO_2$ (Figure 3A). A similar XRD pattern was obtained after the protamine/TiBALDH treatment (Figure 3B), which indicated that the titanium-bearing coating was largely amorphous after deposition. After the thermal treatment (500 °C, 2 h, air), however, the presence of anatase titania was detected by XRD analysis (Figure 3C). After the subsequent NaOH treatment, diffraction peaks for anatase $TiO_2$ were clearly detected in the freestanding structures, whereas the silica diffraction peaks were absent (Figure 3D). Scherrer analysis of the most intense anatase $TiO_2$ diffraction peak in Figure 3D (near $2\theta = 25.3°$) yielded an average anatase crystal size of $6.5 \pm 0.3$ nm. A TEM image of an ion-milled cross-section revealing the pyrolyzed coating on the silica frustule is shown in Figure 4A. SAED analyses of this coating (Figure 4B) was consistent with anatase $TiO_2$. High resolution TEM analyses (Figure 4C) also revealed nanocrystals ($< 10$ nm) with lattice fringes spaced 0.35 or 0.24 nm apart, which were consistent with the (101) and (004) plane spacings, respectively, of anatase $TiO_2$.[14]

We presumed that the binding of protamine to the silica frustule template, and to titania coatings, was strongly influenced by electrostatic interactions. When immersed in aqueous solutions at pH 7.5, the surfaces of silica and titania should be negatively charged,[15] so that the polycationic protamine molecules in such solutions may become electrostatically bound to such surfaces. To investigate whether electrostatic interactions were crucial for protamine binding, two control experiments were conducted in which (i) the pH of the protamine solution

(14) Powder Diffraction File, Cards No. 021-1272 for anatase $TiO_2$, No. 039-1425 for cristobalite SiO2, No. 042-1401 for tridymite $SiO_2$, Newtown Square (PA): International Center for Diffraction Data.

(15) (a) Kosmulski, M. *J. Colloid Interface Sci.* **2006**, *298*, 730–741. (b) Parks, G. A. *Chem. Rev.* **1965**, *65*, 177–198.

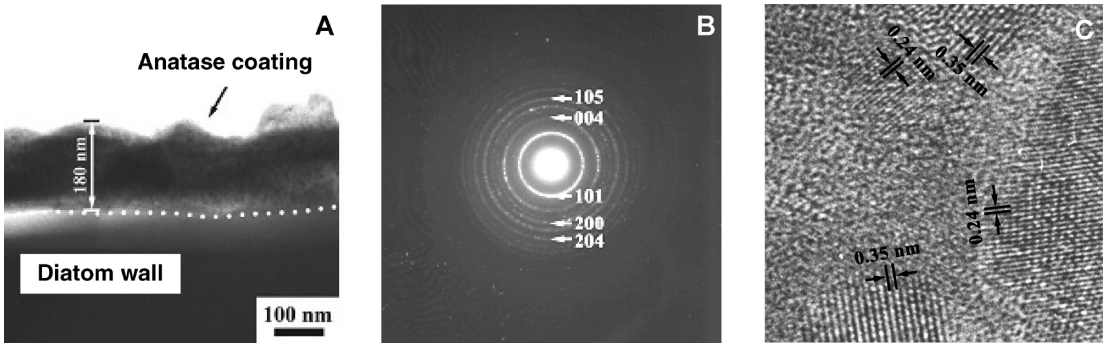


**Figure 4.** Transmission electron microscope analyses of anatase $TiO_2$-coated diatom frustules. (A) Transmission electron microscope image of an ion milled cross-section of a titania-coated *Aulacoseira* frustule after 12 protamine/TiBALDH cycles and firing at 500 °C for 2 h. (B) Selected area electron diffraction pattern obtained from the titania coating shown in (A). (C) High resolution transmission electron microscope image of the titania coating.

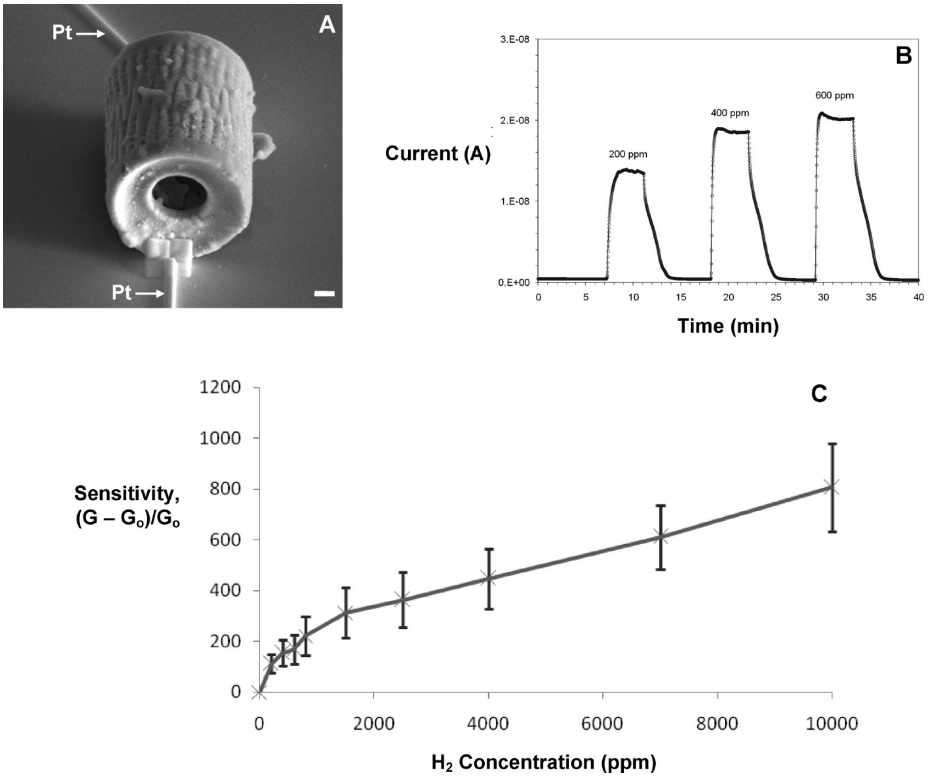


**Figure 5.** Hydrogen gas detection with single titania-coated diatom frustules. (A) Secondary electron image of a titania-coated *Aulacoseira* frustule with Pt connections. (B) Temporal current response upon exposure to gas mixtures with different $H_2$ concentrations. (C) Sensitivity of $TiO_2$-coated frustules to different $H_2$ concentrations. Each data point corresponds to the average of separate measurements obtained from five single, titania-coated frustules. The error range shown for each data point corresponds to ±1 standard deviation about the average value. Scale bar in A: 2 $\mu$m.

in each deposition cycle was lowered from 7.5 to 2.2 or (ii) 1 M NaCl was added to the protamine solution in each deposition cycle, while maintaining the solution pH at 7.5. By lowering the pH of the protamine-bearing solution to 2.2, the concentration of negative charges on the silica and titania surfaces were drastically reduced, which should have substantially decreased the extent of electrostatic binding of protamine to such surfaces. In the presence of a high concentration of NaCl at pH 7.5, the negative charges on the silica and titania surfaces become screened by the $Na^+$ ions, which should reduce the extent of protamine binding to such surfaces. Indeed, energy-dispersive X-ray (EDX) analyses and X-ray diffraction (XRD) analyses of representative *Aulacoseira* diatom frustules that had been exposed to 12 pH-modified or 12 NaCl-modified protamine/TiBALDH deposition cycles and then firing at 500 °C for 2 h revealed a drastic decrease in the titania content relative to frustules coated by the standard process (compare Figures S2A, S2B, S3A, and S3B in Supporting Information with Figures 1E and 3C). These control experiments confirmed the importance of electrostatic interactions between the protamine and the silica and titania surfaces on the layer-by-layer deposition process.

Titania-based sensors have been used to detect a number of gases, including hydrogen, oxygen, carbon

monoxide, and nitrogen dioxide.[16,17] The hydrogen detection capability of single (minimally invasive) titania-coated frustules was examined in this work. After applying platinum electrodes to both ends of a given titania-coated frustule (Figure 5A), the change in current was evaluated upon exposure to varied concentrations of hydrogen gas at a constant bias voltage of 600 mV at 350 °C. The sensing performance of five such single, titania-bearing frustule structures was evaluated. The current carried by each of the single titania-coated frustule sensors exhibited a reversible increase and decrease upon exposure to, and removal of, hydrogen, respectively (Figure 5B). The average response time (i.e., the time required for the measured current to increase to 90% of the peak value) and the average recovery time (i.e., the time required for the measured current to decay to 90% of the peak value) for hydrogen detection at the 200−10 000 ppm concentrations were 62 and 153 s, respectively. The hydrogen sensitivity of the single titania-coated frustule was evaluated upon exposure to $H_2$/Ar gas mixtures containing 200−10 000 ppm $H_2$. The sensitivity, $S$, was defined by the equation:

$$S = (G - G_0)/G_0$$

where $G_0$ is the electrical current flowing through the sensor before exposure to a hydrogen-bearing gas mixture (i.e., in pure flowing argon) and $G$ is the maximum current detected after exposure to the hydrogen-bearing gas mixture. As shown in Figure 5C, the average sensitivity increased monotonically with increasing hydrogen concentration from a value of 113 ± 37 at 200 ppm $H_2$ to a value of 806 ± 172 at 10 000 ppm $H_2$. The response time, recovery time, and sensitivity of the single (minimally invasive) $TiO_2$-coated frustules to hydrogen were comparable to, or better than, those reported for other nanocrystalline or nanostructured $TiO_2$-based hydrogen sensors.[16]

(16) (a) Varghese, O. K.; Gong, D.; Paulose, M.; Ong, K. G.; Grimes, C. A. *Sens. Actuators, B* **2003**, *93*, 338–344. (b) Mather, G. C.; Marques, F. M. B.; Frade, J. R. *J. Eur. Ceram. Soc.* **1999**, *19*, 887–891. (c) Devi, G. S.; Hyodo, T.; Shimizu, Y.; Egashira, M. *Sens. Actuators, B* **2002**, *87*, 12–129. (d) Carney, C. M.; Yoo, S.; Akbar, S. A. *Sens. Actuators, B* **2005**, *108*, 29–33. (e) Chaudhari, G. N.; Bende, A. M.; Bodade, A. B.; Patil, S. S.; Sapkal, V. S. *Sens. Actuators, B* **2006**, *115*, 297–302.

(17) (a) Lu, H. F.; Li, F.; Liu, G.; Chen, Z. G.; Wang, D. W.; Fang, H. T.; Lu, G. Q.; Jiang, Z. H.; Cheng, H. M. *Nanotechnology* **2008**, *19*, 405504/1–405504−7. (b) Kirner, U.; Schierbaum, K. D.; Goepel, W.; Leibold, B.; Nicoloso, N.; Weppner, W.; Fischer, D.; Chu, W. F. *Sens. Actuators, B* **1990**, *1*, 103–7. (c) Guidi, V.; Carotta, M. C.; Ferroni, M.; Martinelli, G.; Paglialonga, L.; Comini, E.; Sberveglieri, G. *Sens. Actuators, B* **1999**, *57*, 197–200.

## Conclusions

The present work demonstrates for the first time that repetitive exposure to a commercially available, multifunctional protein (protamine, which exhibits silica-binding, titania-forming, and titania-precipitating activity) and an aqueous precursor (TiBALDH) can be used to generate a conformal and continuous oxide (titania) coating on a complex, 3-D biosilica template so that, upon organic pyrolysis and selective removal of the template, a freestanding oxide structure is produced that retains the 3-D template morphology. Unlike other wet chemical methods, this simple multifunctional protein-based approach does not require prolonged and/or multistep silica surface functionalization protocols and the coating process can be conducted entirely in water-based solutions at near neutral pH. This process has been used to convert single diatom frustules into minimally invasive and sensitive titania-based hydrogen detectors. With proper selection of the template and template-binding/mineral-forming proteins, this facile conformal coating method may be extended to the fabrication of microscale structures and devices composed of a variety of functional inorganic materials and 3-D morphologies.

**Acknowledgment.** This research was supported by the Office of Naval Research (Dr. Mark Spector, program manager), the Air Force Research Laboratory (Dr. Wallace Patterson, program manager), and the Air Force Office of Scientific Research (Dr. Charles Lee, Dr. Hugh DeLong, program managers). Dr. Joseph M. Slocik (Air Force Research Laboratory, RXBN) is acknowledged for his assistance with XPS analyses. We also wish to thank Emily Malcolm for help with protein isolation.

**Supporting Information Available:** (i) A secondary electron image, EDX analysis, and transmission electron images of Stöber silica spheres containing a conformal and continuous titania coating generated via repeated, alternating exposure of the spheres to protamine-bearing and TiBALDH-bearing solutions at pH 7.5 and (ii) EDX and XRD analyses of *Aulacoseira* diatom frustules after cyclic exposure to protamine-bearing and TiBALDH-bearing solutions, for which the protamine-bearing solution possessed a lowered pH (2.2 instead of 7.5) or contained 1 M NaCl at the standard pH (7.5). The latter (control) experiments were used to evaluate the influence of electrostatic interactions on protamine binding to silica and titania. This material is available free of charge via the Internet at http://pubs.acs.org.